

Performance Analysis of Equivalent-Circuit Topologies for Periodic Leaky-Wave Antenna Asymmetric Radiators

Alberto Hernández-Escobar^{#1}, Elena Abdo-Sánchez^{#2}, Pablo Mateos-Ruiz^{#3}, Jaime Esteban^{*4},
Teresa M. Martín-Guerrero^{#5}, Carlos Camacho-Peñalosa^{#6}

[#]Instituto Universitario de Investigación en Telecomunicación (TELMA), Universidad de Málaga-Andalucía Tech, Spain

^{*}Information Processing and Telecommunications Center (IPTC), Universidad Politécnica de Madrid, Spain

{¹ahe, ²elenaabdo, ³pablomr, ⁵teresa, ⁶ccp}@ic.uma.es, ⁴jesteban@etc.upm.es

Abstract—The traditional problem of broadside radiation degradation in leaky-wave antennas has been overcome in the past years with the introduction of some asymmetry in the radiator. This article analyses the performance of two equivalent-circuit topologies, previously proposed in the literature for asymmetric structures. The aim is to shed some light on the choice of the appropriate circuit when selecting the degree of asymmetry in the unit-cell of periodic leaky-wave antennas. The comparison is carried out through the extraction of the circuit parameters of three different structures and each of them with different degrees of asymmetry.

Keywords—asymmetry, broadside radiation, eigenstates, equivalent circuit, lattice network, leaky-wave antenna.

I. INTRODUCTION

Leaky-wave antennas (LWAs) are excellent candidates for recent applications that require high directivity with low complexity and beam scanning. They consist of a waveguiding structure that leaks power gradually while the wave is being propagated along it. Traditionally, the fundamental problem of periodic LWAs was the performance degradation while scanning through broadside [1]. Nevertheless, many LWAs with broadside effect mitigation have been proposed in the literature, such as [2], [3].

Specifically, it has been shown that the introduction of certain asymmetries in the unit-cell of periodic LWAs can mitigate the so-called open-stopband effect at broadside [4]. In an attempt to elaborate some design methodology to choose the degree of asymmetry needed to cancel the broadside effect, an equivalent circuit was proposed in [4]. It was inspired in the classic symmetric lattice network. Recently, lattice networks have gained more attention [4], [5] due to their unique properties, such as the guarantee of realizability of their elements, or the orthogonal-mode separation. Lattice networks are appropriate for modeling components or discontinuities that have symmetry; however, the extension of this circuit for asymmetric structures is absolutely not straightforward. An alternative to the circuit used in [4] is the equivalent-circuit topology proposed in [6]. Both proposals share the use of some transformers to introduce the required asymmetry, and in both cases unity transformation ratios lead to the degeneration in the symmetric lattice network (the symmetric case). Nevertheless, their element interconnections and parameter derivation follow

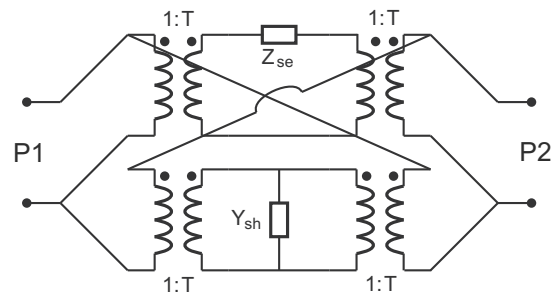


Fig. 1. Transformer-Lattice Network (TLN) for asymmetric structures proposed in [4].

a significantly different approach. The circuit in [6] follows an eigenstate formulation approach and, unlike the circuit in [4], it preserves the property of symmetric lattice networks of being decomposable in eigenstates and guarantees immittances with positive real parts.

The purpose of this communication is to compare the performance of these two equivalent-circuit topologies by analyzing three different LWA unit cells.

II. TOPOLOGIES FOR ASYMMETRIC UNIT-CELLS

A. Transformer-Lattice Network (TLN)

In [4] the classic lattice network is decomposed by means of the well-known Bartlett theorem into its series and shunt immittances. Ideal isolation transformers, with transformation ratio 1 : 1, are then introduced, and the resulting two-port networks are linked in an intricate parallel connection, although unquestionably equivalent to the original lattice. The transformation ratio is then used to break the symmetry and provide an equivalent circuit for non-symmetric structures (see Fig. 1).

The series and shunt immittances of the TLN can be related with the admittance and impedance parameters of the asymmetric structure to be modelled, as follows [4]:

$$Z_{se} = \frac{y_{11} + y_{22} - 2y_{21}}{(y_{21} - y_{11})(y_{21} - y_{22})} \quad (1a)$$

$$Y_{sh} = \frac{z_{11} + z_{22} + 2z_{21}}{(z_{21} + z_{11})(z_{21} + z_{22})} \quad (1b)$$

whereas the transformation ratio is

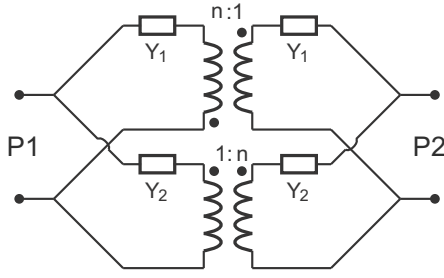


Fig. 2. Eigenstate Lattice Network (ELN) for asymmetric structures proposed in [6].

$$T = \sqrt{\frac{y_{21} - y_{11}}{y_{21} - y_{22}}} = \sqrt{\frac{z_{21} + z_{22}}{z_{21} + z_{11}}}. \quad (2)$$

Obviously, when the structure is symmetric, $T = 1$. In any other case, T is a complex parameter.

B. Eigenstate Lattice Network (ELN)

In [6] the eigenstate formulation approach [7] was adopted. As in [8], two subnetworks are sought for the two eigenvalue excitations of the asymmetric structure and both are linked in a direct parallel connection. The proposed topology for the circuit is reproduced in Fig. 2. Like the symmetric lattice network, this asymmetric version does preserve the eigenstate separation in the branches of the circuit. This property leads to the separation of the even and odd excitations for the case of the symmetric lattice. Additionally, this circuit allows the dissipated power in the branches to be independent of each other and the real parts of the immittances to be always positive, as it also happens in the symmetric lattice network.

Given the eigenvalues λ_1 and λ_2 and the eigenvectors $\mathbf{v}_1 = \frac{1}{\sqrt{p^2+1}}[p \ 1]^T$ and $\mathbf{v}_2 = \frac{1}{\sqrt{p^2+1}}[-1 \ p]^T$, associated to the admittance matrix $[Y]$ of a general passive, reciprocal, two-port network, where

$$p = \frac{(y_{11} - y_{22}) + \sqrt{(y_{11} - y_{22})^2 + 4y_{12}^2}}{2y_{12}}, \quad (3)$$

the network can be decomposed into two subnetworks connected in parallel, each of them corresponding to an eigenstate, as shown in Fig. 2, where $Y_1 = \lambda_1$, $Y_2 = \lambda_2$ (the eigenvalues of the matrix $[Y]$), and $n = 1/p$.

When the structure is symmetric $y_{11} = y_{22}$, $p = 1$, the transformer ratio is $n = 1$, and the ELN becomes a conventional lattice network.

III. COMPARISON BETWEEN TLN AND ELN CIRCUITS

A. The Composite Right/Left-Handed (CRLH) Unit Cell

The first unit cell chosen to perform the comparison, the CRLH from [4], resembles a symmetrical cross, and the asymmetry is introduced by lengthening one of its sides, while shortening the opposite one, a distance d with respect to the symmetric layout, as shown in Figs. 3(a) and 3(c).

Fig. 4 shows the comparison of the TLN and ELN parameters for the CRLH cell for different degrees of

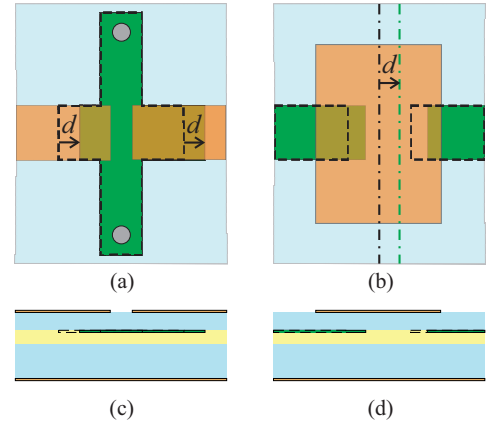


Fig. 3. The CRLH and the SFCP unit cells proposed in [4]. (a) Top view of the CRLH unit cell. (b) Top view of the SFCP unit cell. (c) Side view of the CRLH unit cell. (d) Side view of the SFCP unit cell.

asymmetry simulated using HFSS. To make a fair comparison between the values of the elements of both topologies, T^2 is plotted vs. n , Y_{sh} is plotted vs. Y_1 , and $1/Z_{se}$ is plotted vs. Y_2 , given their similarities. To keep most of the values of the transformation ratios between 0 and 1, their inverses are plotted instead. The maximum misalignment considered in this study is $d = 950 \mu\text{m}$, for which one side of the cross has completely disappeared and the other side is twice the length compared to the symmetric case.

The results showed that, when $d = 0$, both equivalent circuits converge to the same solution (the lattice network), with the transformation ratios, n and T , real with unity value, as expected for the symmetric case. The difference between both equivalent circuits is accentuated for increasing values of misalignment d . Admittance Y_{sh} presents a stronger dependence on d around 6 – 9 GHz than Y_1 , and both show minimal change between the misaligned cases and the symmetric case along the rest of the band. Admittances $1/Z_{se}$ and Y_2 change more among the misaligned cases, although $1/Z_{se}$ shows a pole around 7 GHz, while the ELN counterpart has a smooth behaviour at that frequency and its real part is always positive. Finally, the transformation ratio n evidences a more predictable and monotonous variation with frequency for the ELN. Additionally, the equivalent TLN transformation ratio presents a considerable imaginary part near the resonances, while it is almost irrelevant in the ELN circuit independently of the value of d .

B. The Series-Fed Coupled Patch (SFCP) Unit Cell

The second cell, the SFCP from [4], consists of an on-top-stacked patch with gap coupling to the feeding line, as shown in Fig. 3(b) and 3(d). In this case, the asymmetry results from moving the patch along the feeding line axis.

The simulation results of the SFCP cell are shown in Fig. 5. The maximum misalignment for this cell corresponds to moving the patch a distance $d = 1.675 \text{ mm}$, in which case there would not be any overlapping area between the patch and one of the feeding lines.

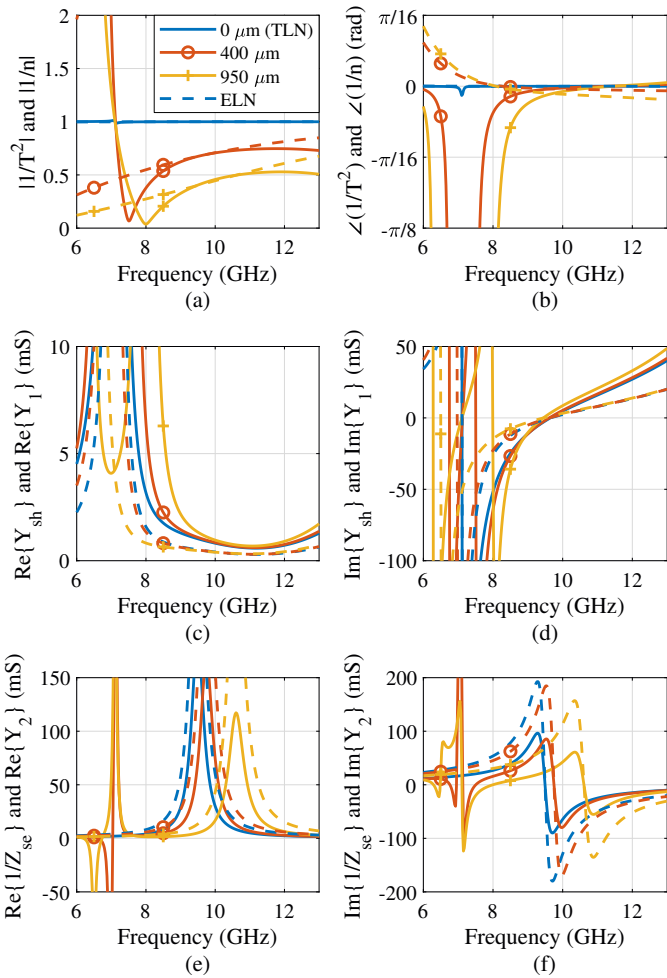


Fig. 4. Extracted T^2 of TLN and n of ELN, (a) and (b), Y_{sh} of TLN and Y_1 of ELN, (c) and (d), Z_{se} of TLN and Y_2 of ELN, (e) and (f), vs. frequency (6 – 13 GHz), for simulated CRLH cells with different degrees of misalignment d . Solid lines represent the TLN and dashed lines the ELN.

In this case, it can be noticed that the values of Y_1 are more akin between the different degrees of misalignment than those of Y_{sh} , which show some ripples that are not present in the symmetric case. Also, the real parts of Y_1 are always real, unlike those of Y_{sh} . Again, the observations obtained for the previous cell's transformation ratios can be applied to this one. T shows resonances along the simulated bandwidth, where the imaginary part becomes relevant (Fig. 5(b)). However, a much smoother solution is achieved for n and its imaginary part is considerably smaller in the entire frequency range.

C. The Misaligned Complementary Strip-Slot

In order to validate the previous comparisons with actual measurements, the *complementary strip-slot* has been chosen as a case study. This structure was proposed by the authors in [5] as a planar radiating element with outstanding broadband matching. Fig. 6 shows a partially backlit photograph of the structure. The misalignment is introduced by moving the strip and the slot a distance $d/2$ towards Ports 2 and 1, respectively.

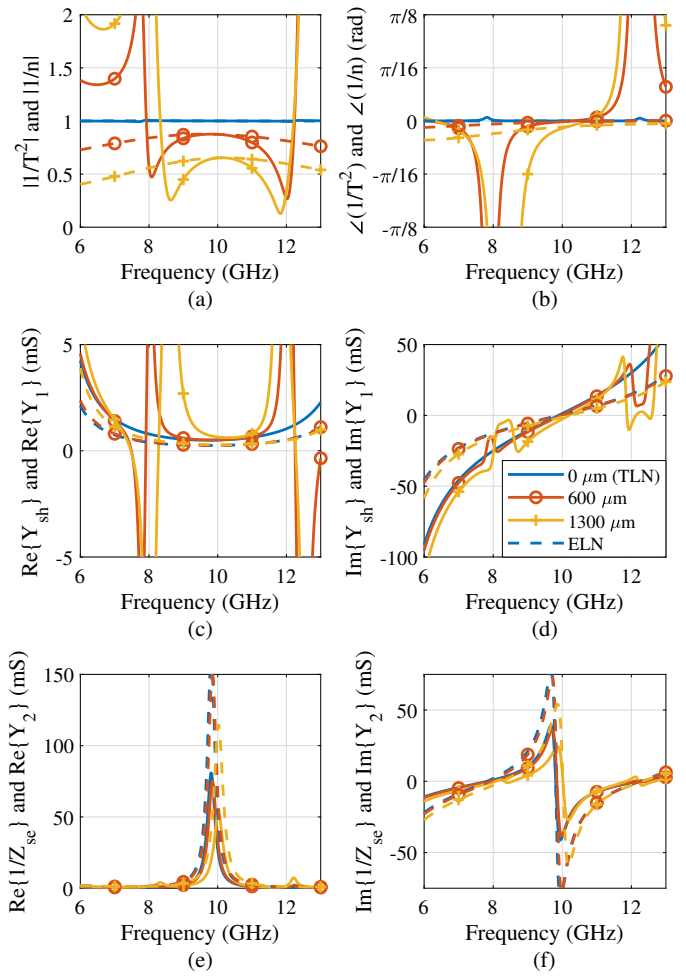


Fig. 5. Extracted T^2 of TLN and n of ELN, (a) and (b), Y_{sh} of TLN and Y_1 of ELN, (c) and (d), Z_{se} of TLN and Y_2 of ELN, (e) and (f), vs. frequency (6 – 13 GHz), for simulated SFCP cells with different degrees of misalignment d . Solid lines represent the TLN and dashed lines the ELN.

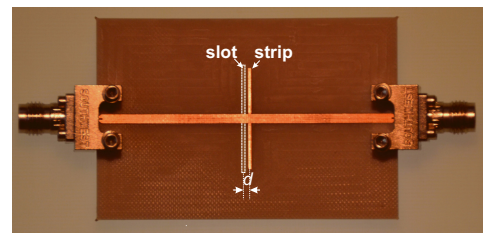


Fig. 6. Backlit photograph of a prototype of the complementary strip-slot with certain misalignment d .

Several prototypes of the strip-slot element with different degrees of misalignment d have been fabricated. Their comparisons of the TLN and ELN parameters are plotted in Fig. 7. To have a reference for the degrees of misalignment analyzed, the case of $d = 540 \mu\text{m}$ corresponds to the minimum value for which the strip and the slot have no overlapping area.

As in previous cases, the differences between both equivalent circuits become relevant when the misalignment is more noticeable. Over the frequency range in which the transformer ratios are close to 1 (around 10 GHz), the behavior

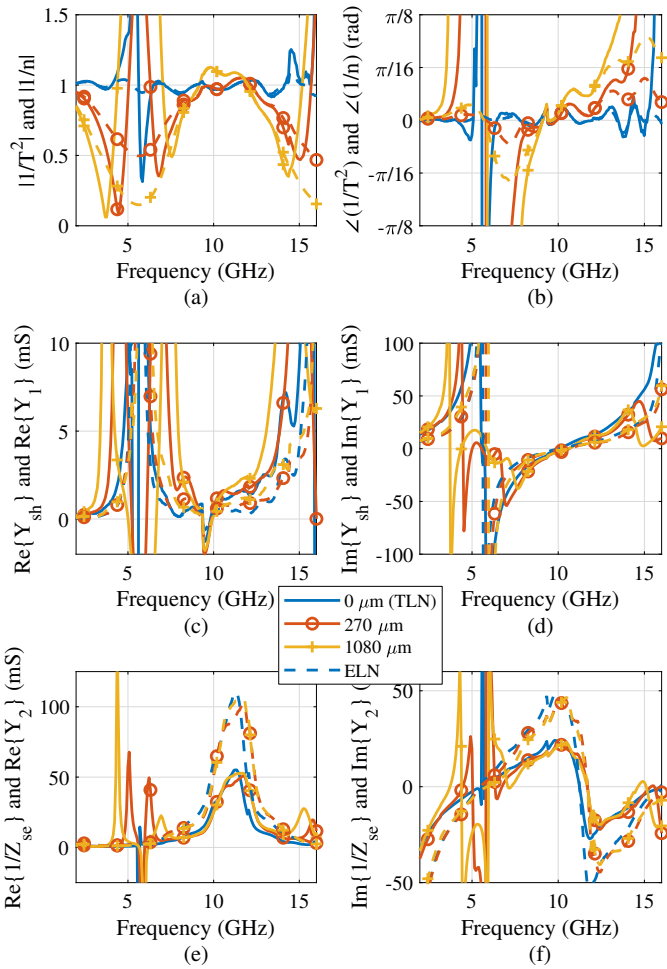


Fig. 7. Extracted T^2 of TLN and n of ELN, (a) and (b), Y_{sh} of TLN and Y_1 of ELN, (c) and (d), Z_{se} of TLN and Y_2 of ELN, (e) and (f), vs. frequency (2 – 16 GHz), for strip-slots with different degrees of misalignment d . Solid lines represent the TLN and dashed lines the ELN.

of the immittances of both circuits is similar. However, out of this band, the impedances of the TLN show a much stronger dependence with the degree of misalignment d than its ELN counterpart. As for the transformation ratios, a smoother variation with frequency is observed for the ELN circuit, which has an oscillatory behavior, being further from the unity near the resonances. This variation has correspondence with the physical behavior of the structure. It can be noticed that, when the structure is asymmetric, the transformation ratio n becomes complex, but its phase remain close to 0 (almost real), even for higher degrees of asymmetry. However, for the TLN, its variation with frequency is more abrupt and unpredictable, and the phase reaches significant values at some frequency ranges.

Therefore, in order to build a LWA with broadside mitigation, the ELN offers a better modeling, since the only parameter that changes remarkably with the degree of asymmetry, over the whole bandwidth, is the transformer ratio. Then, the optimal misalignment could be chosen at any frequency by searching for the transformer ratio required to match the structure. The circuit reveals that a suitable

frequency band to build a broadside LWA with this strip-slot element and with open-stopband mitigation is around 5 – 6 GHz, since the asymmetry has more effect on the transformer in this frequency range. Please note that at this band, the impedances of the TLN are heavily dependent on the asymmetry degree, making much more complicated the choice of the optimal asymmetry. On the contrary, at the band around 10 GHz, the misalignment does not introduce a significant change on the radiator, and then, the use of asymmetry will hardly be sufficient to get good radiation at broadside.

IV. CONCLUSION

In this contribution, two different equivalent circuits for asymmetric structures are compared, in order to analyze their performance when modeling the asymmetry introduced in periodic LWAs to mitigate the broadside effect. Both circuits degenerate in the symmetric lattice network for the symmetric case. The analysis of both circuits for the three unit cells proves that, compared to the TLN, the ELN topology achieves relatively misalignment-independent impedances which have positive real parts, while making the transformation ratio predictable, gradual and with a practically real value. In addition, the ELN has a simpler configuration. Therefore, an eigenstate-based equivalent circuit might facilitate the design of the unit cells of LWAs and be more appropriate for certain structures, as done in [9].

ACKNOWLEDGMENT

This work was supported by MCIU/AEI/FEDER (Programa Estatal de I+D+i Orientada a los Retos de la Sociedad) under grant RTI2018-097098-J-I00 and by the regional government Junta de Andalucía (Spain) PAIDI 2020 under Grant PY20_00452.

REFERENCES

- [1] A. Hessel, "Travelling-Wave Antennas," in *Antenna Theory*, R. E. Collin and F. J. Zucker, Eds. New York: McGraw-Hill, 1969, ch. 19.
- [2] S. Paulotto *et al.*, "A Novel Technique for Open-Stopband Suppression in 1-D Periodic Printed Leaky-Wave Antennas," *IEEE Trans. Antennas Propag.*, vol. 57, no. 7, pp. 1894–1906, July 2009.
- [3] E. Abdo-Sánchez *et al.*, "Short dual-band planar leaky-wave antenna with broadside effect mitigation," *IET Microw., Antennas and Propag.*, vol. 10, no. 5, pp. 574–578, 2016.
- [4] S. Otto *et al.*, "Transversal asymmetry in periodic leaky-wave antennas for bloch impedance and radiation efficiency equalization through broadside," *IEEE Trans. Antennas Propag.*, vol. 62, no. 10, pp. 5037–5054, 2014.
- [5] E. Abdo-Sánchez *et al.*, "Planar Broadband Slot Radiating Element Based on Microstrip-Slot Coupling for Series-fed Arrays," *IEEE Trans. Antennas Propag.*, vol. 60, no. 12, pp. 6037–6042, Dec. 2012.
- [6] A. Hernández-Escobar *et al.*, "An equivalent-circuit topology for lossy non-symmetric reciprocal two-ports," *IEEE J. Microw.*, vol. 1, no. 3, pp. 810–820, 2021.
- [7] S. Wane and D. Bajon, "Broadband equivalent circuit derivation for multi-port circuits based on eigen-state formulation," in *IEEE MTT-S Inter. Microw. Symp. Dig.*, June 2009, pp. 305–308.
- [8] E. Abdo-Sánchez *et al.*, "Equivalent Circuits for Nonsymmetric Reciprocal Two Ports Based on Eigenstate Formulation," *IEEE Trans. Microw. Theory Techn.*, vol. 65, no. 12, pp. 4812–4822, 2017.
- [9] J. Lu *et al.*, "Design of a novel microstrip franklin leaky-wave antenna using the eigenstate approach," *IEEE Trans. Antennas Propag.*, vol. 67, no. 7, pp. 4484–4494, July 2019.